A Novel Ultrasonic Doppler Fetal Heart Rate Detection System Using Windowed Digital Demodulation

MING DAI[ID][1,2], KAI ZHAN[3], RONGCHAO PENG[4], JINFENG XU[1,5], HUI LUO[ID][1,5], YINGYING LIU[1,5], LIANGPING LUO[6], HUIYING WEN[7], AND SIPING CHEN[7]

[1]Department of Ultrasonography, Shenzhen People's Hospital, The Second Clinical Medical College, Jinan University, Shenzhen 518020, China
[2]Department of Artificial Intelligence, Shenzhen Polytechnic, Shenzhen 518055, China
[3]JOINTO Technology Company Ltd., Changsha 410000, China
[4]School of Biomedical Engineering, Guangdong Medical University, Dongguan 523808, China
[5]Shenzhen Medical Ultrasound Engineering Center, Department of Ultrasonography, Shenzhen 518020, China
[6]The First Affiliated Hospital of Jinan University, Guangzhou 510632, China
[7]Health Science Center, School of Biomedical Engineering, Shenzhen University, Shenzhen 518060, China

Corresponding authors: Jinfeng Xu (xujinfeng@yahoo.com), Hui Luo (luoh98@sina.com), and Yingying Liu (yingyingliu@ext.jnu.edu.cn)

ABSTRACT Fetal heart rate (FHR) is an essential indicator of fetal well-being. The ultrasonic Doppler FHR detector is widely used to monitor the fetus's health due to its advantages of non-invasion, high sensitivity, and good directivity. However, the existing commercial Doppler FHR detector primarily uses an analog multiplier for demodulation, which has limited functions and insufficient sensitivity. The analog demodulation is performed only on a single-sideband signal(in-phase or quadrature) (IQ), which is impossible to derive the fetal heart movement's vector velocity. Moreover, repetitive recognition of the mitral valve's positive and negative motion easily causes the measured FHR twice the actual one (FHR doubling). Although the traditional digital demodulation FHR detector can obtain in-phase and quadrature demodulation signals, it needs a high-level field-programmable gate array chip and therefore cannot meet low-power consumption requirements in battery-powered situations. Herein we proposed a novel digital demodulation FHR algorithm using time-domain windowing. Then, we applied the algorithm into a low-power complex programmable logic device to achieve low-cost acquisition of vector velocity and suppress FHR doubling and finally designed a hand-held, noninvasive digital Doppler FHR detection system for continuous perinatal detection. In this work, the comparison curve between the TREND curve generated by the simulator and the measured curve of our FHR detector was obtained. The comparative experiment between the commercial FM-3A FHR detector and our proposed FHR detector was performed, and the relative error and standard error of the obtained FHR data were used to evaluate the two FHR detectors' detection accuracy. The results showed that our FHR detector showed excellent detection accuracy at an accuracy rate of 98%, which was much higher than the average accuracy of the FM-3A FHR detector and indicated our proposed digital FHR detector showed excellent detection performance. It means that the proposed digital windowed FHR demodulation algorithm is practical, the multi-FHR monitoring system is feasible, and our proposed FHR detector has high detection accuracy, effectively suppresses FHR doubling, and meets the requirements of Chinese national standards. It provides an alternative scheme towards the low-cost hand-held digital demodulation FHR detection application.

INDEX TERMS Windowed algorithm in time-domain, digital demodulation, low-power wireless FHR detection, multiple FHR monitoring.

The associate editor coordinating the review of this manuscript and approving it for publication was György Eigner[ID].

I. INTRODUCTION

According to statistics from the center for disease control and prevention, a total of 23,595 fetal deaths at 20 weeks of

gestation or more were reported in America in 2013, and the fetal mortality rate was 5.96 fetal deaths at 20 weeks of pregnancy or more per 1,000 live births [1]. It was estimated that over one million fetal deaths take place in America per year [1]. Premature delivery, hypoxia, intrauterine growth retardation, or other complications cause fetal distress and neonatal death and lead to risks to pregnant women's health. Therefore, it is of great significance to dynamically monitor the fetus and gravida's health status during the pregnancy. It is often used to reflect the autonomic nervous system's development, physiological activity, and fetal health status [3]. For example, FHR is regulated by the autonomic nervous system, specifically by way of the sympathetic and the parasympathetic nervous system, and it is closely related to the pregnancy cycle. The normal FHR is about 110-160 beats per minute (BPM) [4], and the average FHR before 20 weeks of pregnancy is about 162 BPM. The average FHR at 21-30 weeks of pregnancy is approximately 147 BPM and the average FHR at 31-40 weeks of pregnancy is around 139 BPM. When the pregnancy is 12 weeks, the FHR can be as high as 170 BPM, and when the pregnancy exceeds 40 weeks, the FHR can be lower than 110 BPM. Therefore, when the FHR measurement time is more than 10 minutes, and the pregnant woman's FHR is higher than 170 BPM or lower than 110 BPM, it is usually considered an obvious FHR abnormality, often caused by fetal hypoxia, ischemia, and other factors. Once fetal severe hypoxia or ischemia occurs, it is effortless to cause congenital disabilities, even fetal death. Therefore, it is crucial to obtain the FHR of pregnant women accurately. To improve the quality of fetal delivery, reduce fetal mortality, inhibit the birth of congenital disabilities and mentally retarded fetuses. Investigating and designing an electronic FHR detection system used in hospitals, community health centers, and various healthcare settings to provide high-accurate FHR detection is meaningful. An ambulatory FHR detection system that can be used for accurate long-term monitoring of FHR and can be applied to prevent fetal hypoxia and identify symptomatic signs for pregnant women with abnormal FHR conditions is urgently needed.

As the electronic FHR monitoring system can effectively prevent fetal hypoxia, allow optimal timing of delivery, gain maximum fetal maturity, and avoid intrauterine fetal death [5], more and more attention has been paid to the development of electronic FHR monitor in last few decades to optimize and improve the fetal and maternal outcomes during pregnancy, labor, and delivery [6]. For instance, the electronic FHR monitoring technology by adopting an abdominal electrocardiogram method of continuously recording FHR was first introduced by Edward in 1958 [7], making the FHR monitoring stride into a new era. Free-man et al. reported that changes in the fetal heart waveform might correlate with hypoxia [8]. In the 1950s and 1960s, the technologies of phonocardiography, abdominal electrocardiogram, and toco-dynamometers were used by the research teams of Caldeyro-Barcia, Hammacher, and Hon to investigate visual tracings of FHR changes, including bradycardia, variability, tachycardia,

and the relationship of these tracings to fetal distress. In 1968, the first commercial fetal monitor was invented by Hewlett Packard [9]. Subsequently, electronic FHR monitoring has been gradually applied to FHR detection to check the baby's health [10]. In the following decades, computer-assisted analysis of cardiotocograph recordings has been introduced [11], [12]. New methods of computerized FHR analysis and electrocardiogram have been developed [10]. Other technologies, including fetal magnetocardiography [13], fetal photoplethysmography [14], fetal cardiotocography, and phonocardiography, are also promising fetal monitoring techniques. Although FHR can be obtained by various technologies [15] [16], the method based on the ultrasonic Doppler effect for detecting the FHR is a noninvasive practical approach. Therefore, the electronic FHR detection system using the ultrasonic Doppler effect has been widely and intensively researched worldwide and achieved widespread application. For instance, Doppler ultrasonography was used to determine the typical ranges of computerized FHR parameters by Simone Breukelman et al. in 2005 [17]. Ahmet Mert et al. denoted that reliability and accuracy are two performances of Doppler-based FHR monitor that need to be improved in 2015 [18]. The technology of Doppler ultrasonography for continuous FHR monitoring and intermittent FHR measurements was described by Paul Hamelmann et al. in 2019 [16]. Additionally, Doppler ultrasound (DUS) devices have been widely used for several decades to estimate FHR. In Doppler ultrasound devices, the primary disadvantage of DUS is the high sensitivity to fetal movement as the detection of FHR mainly relies on the correct positioning of the ultrasound probe, time intervals of the cardiac events are often estimated from the DUS signal by using several methods such as digital filtering, short term Fourier transform, or wavelet analysis. The autocorrelation (AC)-based approaches are often adopted as a computationally inexpensive approach and are often used to identify the dominant frequency. However, AC-based methods are affected by the inherent smoothing or averaging of the autocorrelation. Therefore, Valderrama et al. introduced a reproducible and generalizable AC-based method for FHR estimation from one dimensional Doppler ultrasound (1D-DUS) signals taken with an inexpensive handheld FHR detector [19]. Al-Angari et al. proposed the use of empirical mode decomposition (EMD) of the 1D-DUS signals and the kurtosis of the instantaneous mode function as a measure of FHR. They proved the EMD-kurtosis method derived higher accuracy than AC-based methods. However, the EMD-kurtosis method parameters were optimized using all of the datasets, resulting in likely overfitting on the limited data [20]. Alnuaimi et al. adopted a swarm decomposition method to estimate fetal cardiac intervals. They obtained an excellent identification of the fetal cardiac timing events by adopting the cepstrum analysis method to analyze the fetal Doppler signal. In their experiments, the component linked to valve movements was separated by applying the cepstrum analysis method, and the peaks that correspond

to specific cardiac events were divided. However, the quantitative comparison with the pulsed wave Doppler image-based valve motion timings was not provided with the offered data. Although the presented DUS cepstrum analysis method allows efficient identification of the cardiac events that preserve physical meaning, the technique's primary drawback is its time complexity. Thus, it is still not suggested for real-time applications [21]. Subsequently, Katebi *et al.* proposed a probabilistic segmentation method enabled by a hidden semi-Markov model, which was regarded as an unsupervised approach along with the use of spectral and temporal features as an input to a clustering algorithm, significantly improved DUS segmentation and heart rate variability assessment. They presented one of the most accurate approaches for the beat-to-beat monitoring of fetuses using 1D-DUS signals [22]. The above methods are based on limited data sets. Both the fetal ECG and DUS data are simultaneously recorded and digital signals are processed using offline processing methods. Several optimized FHR detection algorithms are also used to detect fetal heart valve movements from 1D-DUS recordings. However, they require simultaneous fetal ECG as a reference. Most importantly, the optimized FHR algorithms have not yet been applied to chip-based designs, and hand-held 1D-DUS devices based on digital demodulation have never been reported.

Although tremendous achievements were made in the past several decades, several technical limitations such as the inaccurate beat-to-beat estimation of the FHR in the traditional analog Doppler FHR detector (Doppler transducer) [23], high-cost and high power consumption in the traditional digital Doppler FHR detector (Doppler imaging technique), need further investigation. Those issues make low-cost and high-accuracy FHR detection full of challenges. Although the traditional analog FHR detectors have been widely used in the market and have high-cost performance and low-power consumption, the comprehensive sensitivity is not high. It is hard to obtain a high-SNR FHR curve due to maternal heart signal interference, maternal respiratory sounds, maternal motion, maternal digestive sounds, nonlinear transmission medium, acoustic noise produced by fetal movements, movements of the maternal abdominal surface sensor during detection, and ambient noise [24], [25]. Additionally, the traditional analog FHR detectors have inferior stability, low detection precision, and they are hard to distinguish FHR doubling (the measured FHR is twice the actual FHR). Both the function and the monitoring of early gestation fetus are limited, and they only extract the in-phase signal (I signal) or orthogonal signal (Q signal). That means the traditional analog FHR method cannot obtain the full fetal heart motion information [1]. The development of the Doppler FHR monitor based on analog demodulation is incredibly restrained. Therefore, more advanced FHR monitoring methods need to be developed to reduce the false-positive rate for compromised babies' prediction [10].

As electronics and sensors have rapid developed over the past several years, more cost-effective approaches have been proposed to replace traditional analog FHR demodulation methods for FHR monitoring. The ultrasonic Doppler FHR detection technologies are developing towards portability, miniaturization, and high detection precision. It was then the traditional digital FHR detectors appeared and have been developed. However, as the traditional digital FHR demodulation algorithm generally needs a high-level field-programmable gate array (FPGA) chip, yet the FPGA chip cannot meet low-power and low-cost requirements. Besides, the traditional digital FHR detectors (digital demodulation FHR detection devices based on Doppler ultrasound) such as Philips iu22, GE VIVID7, are multi-functional, can detect the vector velocity of fetal heart movement, distinguish the direction of fetal heart movement and inhibit the FHR doubling. However, they are expensive, and require skilled specialists to operate and are only performed for particular cases of fetal and maternal conditions. Besides, they are often large, non-handheld, high-power, and cannot be widely used by ordinary people. So the use is restricted by the place. Therefore, we proposed a novel windowed digital demodulation algorithm that is different from the traditional digital FHR demodulation algorithm and has many advantages. For example, the hardware logic resource required for our proposed algorithm is about 4% that of the traditional digital FHR demodulation algorithm, which makes it possible to realize digital FHR demodulation on a low-cost and low-power complex programmable logic device (CPLD). It also provides the possibility of developing a low-cost, noninvasive wireless digital FHR monitoring system. Most importantly, the fetal heart's vector kinematics parameters are expected to be obtained, and the heat dissipation and power consumption of the chip are hopeful of reducing effectively. The FHR doubling is expected to be overcome effectively.

This paper presents a novel demodulation method based on time-domain windowing as digital FHR demodulation algorithm for miniaturization, convenience, and accuracy of FHR measurement, a hand-held wireless ultrasonic Doppler detector using the demodulation algorithm is designed, and comparative experiments between the FM-3A FHR detector and our proposed FHR detector were carried out. In this study, our presented wireless FHR detection system focuses on the low-cost, low power consumption, and overall performance of the digital FHR detection system to increase the battery life and achieve a low-cost and accurate acquisition of vector velocity of fetal heart movement. Additionally, a miniaturized digital multi-FHR monitoring system for multiple FHR detection was designed and implemented to reduce FHR monitoring costs in this work.

II. FHR DETECTION PRINCIPLE OF AND DEMODULATION METHODS
A. FHR DETECTION PRINCIPLE
When relative motion between sound source and object occurs, the reflected ultrasound's frequency changes lead to Doppler frequency shift, which can be applied in detecting FHR. When the ultrasonic probe transmits the

excitation signal and couples into the maternal abdomen through the coupling agent, the excitation ultrasound encounters the beating fetal heart. Subsequently, the reflected ultrasound echo can be received through the ultrasonic probe. Then the Doppler frequency shift can be derived by computing the frequency difference between the transmitted ultrasound wave and the received ultrasound signal. According to the Doppler frequency shift principle [18], the fetal heart velocity *v* is written as:

$$v = \frac{f_d \cdot c}{2f_1 \cos\theta} = \frac{(f_2 - f_1)c}{2f_1 \cos\theta} \quad (1)$$

where θ, f_1, f_2, f_d, c represent the angle θ between the ultrasonic probe and the fetal heart movement direction, the ultrasonic excitation frequency, the echo receiving frequency, Doppler frequency shift, and ultrasonic propagation velocity within a tissue, respectively.

By obtaining the above five parameters, the velocity of the fetal heart can be calculated by Eq. (1). We can see that the ultrasonic frequency shift is proportional to the velocity of fetal heart movement. When the velocity $v > 0$, i.e., $f_2 > f_1$, the FHR is diastoleing; when the velocity $v = 0$, the FHR is at rest, while when the velocity $v < 0$, the FHR is contracting, the above phenomenon denoted that velocity change can be used to represent the variation of fetal heart movement. As the velocity periodically changes with time, the FHR can be derived by analyzing the fetal heart's velocity.

B. FHR DEMODULATION METHODS
1) TRADITIONAL ANALOG FHR DEMODULATION
In the traditional analog FHR demodulation process, assuming the ultrasonic excitation signal to the ultrasound transducer $f_T = A_1 \sin(f_1 t + \varphi_1)$, the ultrasonic echo signal can be denoted as $f_R = A_2 \sin(f_2 t + \varphi_2)$.

where A_1, A_2 are the amplitudes of two signals, f_1, f_2 are the frequencies, φ_1, φ_2 are the initial phases, and Δf is the frequency variation (i.e., $\Delta f = f_2 - f_1$).
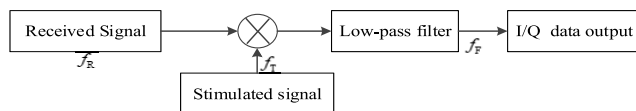

FIGURE 1. Traditional analog FHR demodulation.

As the same transducer is used both in the excitation and reception processes, the probe is tightly positioned on the maternal abdomen, which means that the phase difference between the ultrasonic excitation signal and ultrasonic echo signal can be ignored. After the analog mixing of the stimulated signal and the received signal is carried out, low-pass filtering is then performed on the mixed-signal. As the analog FHR demodulation is a single sideband demodulation method, I/Q signal can be expressed as $f_F = \frac{1}{2}A_1A_2 \cos[(\Delta f)t]$. The traditional analog FHR demodulation is shown in Fig. 1.

2) TRADITIONAL DIGITAL FHR DEMODULATION
The traditional digital FHR demodulation algorithm usually includes five steps:
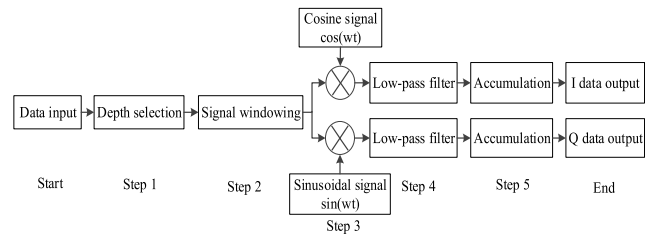

FIGURE 2. Traditional digital FHR demodulation.

- Step 1: Depth selection;
- Step 2: Signal windowing;
- Step 3: Digital signal multiplication;
- Step 4: Low-pass filtering;
- Step 5: Signal accumulation;

The traditional digital FHR demodulation is shown in Fig. 2. The first step is to obtain the ultrasonic echo signal of the specified depth. To avoid the Gibbs phenomenon in the frequency-domain, the truncated segments of the ultrasonic echo signal in the time-domain are windowed in step 2. Subsequently, the windowed signal is divided into two channels, and then they are mixed with the two signals; one signal(I) is the carrier with the same frequency and the same phase, and the other signal(Q) has a phase difference of 90 degrees with the former. After that, the mixed-signal, including multiple frequency signal and envelope signal, are obtained in step 3, and then, the frequency doubling signal is filtered out by a low-pass filter in step 4. Finally, data in buffer are accumulated to derive the I signal and the Q signal in step 5.
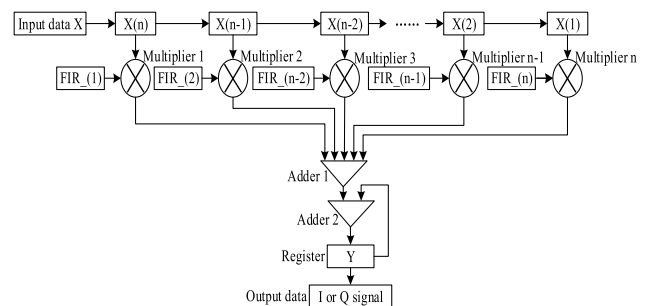

FIGURE 3. FIR filtering and accumulation process.

As shown in Fig. 2, each step of traditional digital FHR demodulation is carried out separately, which results in some idle and waste of hardware logic resources. For example, FIR multistage multipliers are generally utilized as parts of the low-pass filter to filter out the frequency doubling signal in step 4. However, the signal envelope is usually obtained by accumulating all multipliers in the FIR filtering process, which leads to a waste of hardware logical resources due to many multiplications. The above FIR filtering and accumulation process can be described in Fig. 3.

In Fig. 3, *X* is expressed as the input signal after mixing processing, *n* represents the FIR filter length, *X* (1) to *X* (*n*) are denoted as *n* registers. Besides, Fir_ (1) to Fir_ (*n*) are

depicted as the FIR filter parameter, Mult_ 1 to Mult_ n are n multipliers, and Adder 1 is denoted as an n-order adder. In the FIR filtering and accumulation process, input data is sent to X (1) to X (n) by shift, then the data obtained by multiplying X (n) and Fir_ (n) is sent to the multiplier n, and then by accumulating Multiplier 1 to Multiplier n is to realize the function of FIR low-pass filter. Besides, Y(n) is a register that can store the data obtained by Adder 2, and then the data is sent back to Adder 2 again to realize the function of accumulation in step 5. Finally, the signal I or signal Q can be obtained after the above process. As can be seen from Fig. 2 and Fig. 3, the implementation of the traditional digital FHR demodulation algorithm involves many multipliers and accumulators, which consumes many hardware logic resources. It is generally carried out on FPGA level chips for conventional digital FHR demodulation to perform real-time digital processing. As the FPGA chip has a higher cost and higher power consumption, it isn't easy to satisfy the portable FHR detection system's power consumption in a battery-powered scenario. Therefore, if the traditional digital FHR demodulation algorithm can be optimized to reduce the demand for logical hardware resources, we can apply it to a low-cost CPLD chip. It is expected to achieve a low-power consumption and high detection accuracy FHR detector. It will be beneficial to us and expected to promote a significantly digital FHR detector application, especially for the wireless FHR monitor.

3) DIGITAL FHR DEMODULATION USING TIME-DOMAIN WINDOWING

To overcome the traditional digital FHR detector's shortcomings, we proposed a time-domain windowed digital FHR demodulation algorithm. Our proposed demodulation algorithm is based on the conventional digital FHR demodulation algorithm. The derivation process is as follows.

As shown in Fig. 2, we set X as the received ultrasonic signal matrix after depth selection, n is denoted as the length of the matrix, G represents the windowed function matrix in step 2, $g(n)$ is expressed as the coefficient of the windowed function. The matrix P after signal windowing can be expressed as:

$$P = XG \tag{2}$$

where

$$G_{i,j} = \begin{bmatrix} g(i) & \text{if } i = j \\ 0, & \text{if } i \neq j \end{bmatrix}_{(n,n)}$$

Then, mixing processing is carried out in step 3, in this part, assuming matrix C is the in-phase trigonometric function matrix. And then, the result of mixing processing can be simplified as:

$$D = PC$$
$$C_{i,j} = \begin{bmatrix} \cos\{\omega[t+(i-1)\Delta t]\}, & \text{if } i = j \\ 0, & \text{if } i \neq j \end{bmatrix}_{(n,n)} \tag{3}$$

$\Delta t = \frac{2\pi f}{f_{sample}}$, f is the carrier signal frequency, f_{sample} is the sampling frequency, both i and j are integers, and $i \leq n, j \leq n$.

As can be seen from Fig. 2, step 4 is the low-pass filtering, which aims to remove the frequency, which is twice the input signal's frequency, and obtain the envelope signal. In this part, Y is set as the sequence signal after low-pass filtering, F is denoted as a group of filters with the length of n, and $d(1)$ to $d(m+l)$ are the received ultrasonic signal's intercepted fragments obtained by signal windowing, which can be shown in Eq. (3), and then they are used to conduct the convolution operation with FIR low-pass filter coefficient $f(1)\cdots f(n)$, after the low-pass filtering, we can derive Y, which can be denoted as

$$Y = DF \tag{4}$$

where $m+l$ is equal to the length of the received ultrasonic signal, i.e., $m+l = n$, F is the FIR filter coefficient matrix.

As a result, the accumulation process of step 5 can be represented as

$$I = YE \tag{5}$$

where $E = [11111\ 1...1]'_{(1,m)}$, m is an integer, and $m \leq n$.

Therefore, the whole digital FHR demodulation process can be expressed as

$$I = XGCFE \tag{6}$$

Assuming $Z = GCFE$, then $I = XZ$ according to the properties of matrix operation.

Meanwhile, matrix S can be set as the orthogonal trigonometric function matrix, matrix Q is the output orthogonal matrix, and assuming $Z = GSFE$, then $Q = XZ$.

In the digital FHR demodulation process, as G, C, S, F, E are known in advance. Therefore, the traditional digital FHR demodulation can be simplified to multiply the input matrix X and the demodulation matrix Z, which can be easily realized by a multiplier and two accumulators. The circuit block diagram of the digital FHR demodulation algorithm using time-domain windowing is shown in Fig. 4.

Therefore, the time-domain windowed digital FHR demodulation algorithm flow diagram can be simplified as Fig. 5. Like the traditional digital FHR demodulation approach, depth selection of ultrasonic echo signal is also be performed in our time-domain windowed digital FHR demodulation. After depth selection, the windowed sequence of I signal and windowed sequence of Q signal are obtained, then through data accumulation by Add_I and Add_Q, both I signal and Q signal is derived. Compared with the traditional digital FHR demodulation algorithm, our proposed algorithm dramatically reduces the occupation of digital logic resources, cuts down the circuit complexity, and decreases chip power consumption. Therefore, it is possible to apply it to a low-cost CPLD chip.

Besides, to obtain the vector velocity of the fetal heart movement, the mean value of angular frequency should be
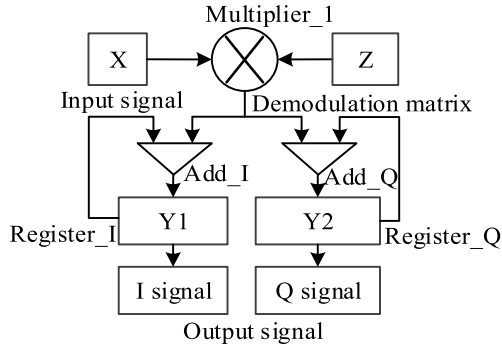
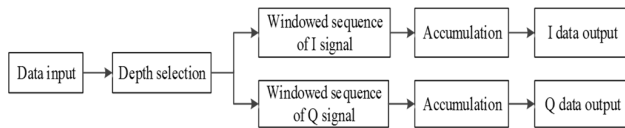**FIGURE 4.** Circuit block diagram of digital FHR demodulation algorithm using time-domain windowing.

FIGURE 5. Algorithm flow diagram of time-domain windowed digital FHR demodulation process.

obtained first [26], and it can be written as

$$\bar{\omega} = \frac{\int_{-\infty}^{+\infty} \omega P(\omega)d\omega}{\int_{-\infty}^{+\infty} P(\omega)d\omega} \quad (7)$$

where ω is the angular frequency, $\bar{\omega}$ is the mean value of the angular frequency, $P(\omega)$ is the power spectral density.

Moreover, the extraction of the velocity of the fetal heart movement usually depends on the average angular velocity[26], which is given by

$$v = \frac{\bar{\omega}}{2\pi f_1} \frac{c}{2} \quad (8)$$

where v is the velocity of fetal heart movement, f_1 is the ultrasonic excitation frequency, and c is the speed of ultrasonic propagation.

As each fetal heart signal in complex coordinates can be regarded as the composition of two orthogonal signals, the complex digital signal can be expressed as Eq. (9) [26].

$$r(i) = x(i) + jy(i) \quad (9)$$

where $r(i)$ is the complex digital signal, $x(i)$ is the real part, and $y(i)$ is the imaginary part.

Combined with Eq. (7) $\sim$ (9), the vector velocity of fetal heart movement can be expressed by Eq. (10) [27].

$$v = -\frac{c}{4\pi f_1 T_p} \arctan\left[\frac{\sum_{i=1}^{N-1} y(i)x(i-1) - x(i)y(i-1)}{\sum_{i=1}^{N-1} x(i)x(i-1) + y(i)y(i-1)}\right] \quad (10)$$

where the ultrasonic excitation frequency f_1 is 1 MHz, T_p is the pulse repetition period.

In our proposed digital FHR demodulation method, the calculated velocity contains the velocity of fetal heart movement and the direction of fetal heart movement. Therefore, the

time-domain windowed digital FHR demodulation can effectively prevent FHR doubling and obtain accurate fetal heartbeat. Besides, our proposed digital FHR demodulation algorithm has the advantages of traditional digital FHR demodulation. It can effectively economize the chip's hardware logic resources and reduce power consumption. Therefore, it provides the possibility to realize a low-cost, low-power consumption, and high detection precision FHR demodulation detector in the future.

III. DESIGN OF DIGITAL MULTI-FHR MONITORING SYSTEM

Although the traditional ultrasonic Doppler FHR monitor has been widely used due to its low-cost, low-power consumption, and non-invasion, it cannot analyze the vector velocity of fetal heart movement. The mitral valve's positive and negative movement is repeatedly recognized, which extremely likely leads to the FHR doubling. While the traditional digital Doppler FHR monitor can accurately obtain the IQ signal, it generally requires a high-level FPGA chip, which cannot meet the requirements of low-power consumption and high cost-performance. It also means that the traditional digital demodulation cannot be applied to wireless Doppler FHR monitor in battery-powered situations. Based on this, we propose a time-domain windowed digital FHR demodulation algorithm in this paper, which can effectively save hardware logic resources and reduce the chip's power consumption. Therefore, it is expected to solve the problem that the traditional digital FHR demodulation cannot realize portable FHR monitoring through the battery power supply.

Additionally, to reduce the cost of monitoring and realize the real-time synchronous tracking, analysis, and abnormal FHR warning of multiple pregnant women, we designed a multi-FHR monitoring system for simultaneous detection of FHR of up to 32 pregnant women. The multi-FHR monitoring system comprises several wireless FHR detectors and an FHR monitoring host, and each pregnant woman in the same community or the same hospital holds one wireless FHR detector. Each detector is placed on the corresponding fetal heart position of each pregnant woman. The common fetal heart monitoring host synchronously collects the wireless FHR detectors' fetal heart data, and then it can analyze, monitor, and issue abnormal FHR warnings.

A. DESIGN OF WIRELESS DOPPLER FHR DETECTION SYSTEM

As the primary research of this study, the wireless ultrasonic Doppler FHR detection system mainly contains four components: 1) ultrasonic excitation and acquisition circuits, 2) CPLD digital signal processing circuits, 3) MCU and peripheral circuits, 4) system software. The ultrasonic excitation and acquisition circuits can be divided into ultrasonic excitation circuits and echo receiving circuits. The former circuits include driving signal amplification, impedance matching, and excitation signal generation, while the latter circuits contain ultrasonic echo amplification, hardware filtering, and
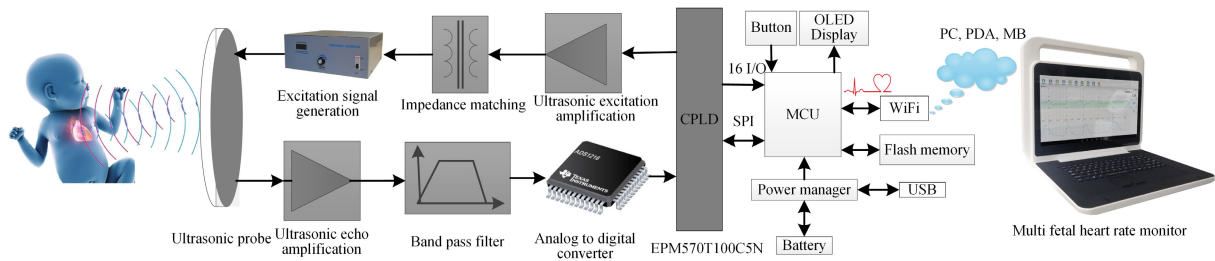
FIGURE 6. Overall structure frame of our proposed wireless FHR detection system.

analog to digital conversion. Firstly, in this work, the burst pulse signal is generated by the CPLD timing control circuit, and the ultrasonic excitation signal is generated after power amplification of driving signal and impedance transformation. Then the generated excitation signal is acted on the ultrasonic probe. Subsequently, the ultrasonic echo signal is received by the transducer. After the ultrasonic echo amplification, band-pass filtering, and analog to digital conversion, the echo signal is then sent to the CPLD digital signal processing unit to conduct digital filtering and time-domain windowed FHR demodulation. After that, we can obtain the IQ demodulation signals and vector velocity of the fetal heart movement. Finally, the fetal heart information detected by the wireless FHR detector is transmitted to an upper-computer (UC) through a wireless communication module for further analysis, processing, storage, and display. During that process, personal computer (PC), personal digital assistant (PDA), mobile phone (MB), the multi-FHR monitoring host can be treated as the UC. To realize a multi-to-one connection between the wireless FHR detectors and the UC, ZigBee, Bluetooth, and WiFi are often used to complete the connection function. WiFi can satisfy the data bandwidth and pairing number requirements, it can transmit the fetal heart data smoothly, in realtime, for long distance, and in low latency. Therefore, a WiFi chip named ESP8266 is used to realize wireless data transmission in our design. Additionally, to reduce the power consumption as much as possible, an ultra-low-power microcontroller unit (MCU), STM32F103RCT6 manufactured by ST Corporation, is selected as the microprocessor. A 2500 mAH, 3.7 V polymer lithium battery, and a battery protection circuit are included in our wireless FHR detection system.

The control circuit consists of MCU and peripheral circuits composed of OLED display, button, WiFi, power manager, flash memory, battery, and universal serial bus (USB). The overall structure frame of the wireless FHR detection system is shown in Fig. 6.

Moreover, our proposed wireless FHR detection system is based on the Doppler frequency shift. STM32F103RCT6 is utilized as a timing control MCU, which controls the CPLD chip (EPM570T100C5N, Altera Inc., USA) to generate a burst excitation pulse with a repetition rate of 2 kHz, 40 cycles of sinusoidal waves, and center frequency of 1 MHz. After driving signal amplification and impedance matching,

an ultrasonic excitation wave is generated and acted on an ultrasonic probe. The probe is then placed on the maternal abdomen, and then the ultrasonic excitation signal is emitted to the fetal heart through the ultrasonic coupling agent. When the ultrasonic excitation signal meets the moving heart wall, it produces reflection and scattering, which leads to a forward or reverse Doppler frequency shift. By filtering and amplifying the ultrasonic echo signal and passing through a 10-bit high-speed ADC acquisition, the digitized ultrasonic echo signal is obtained by the CPLD chip. Subsequently, the CPLD conducts digital filtering and demodulation processing on the digitized ultrasonic echo signal. After that, fetal heart data such as the Doppler frequency shift signal, vector velocity are obtained by adding a time-domain window, multiplication, and accumulation. Finally, the FHR is derived by analyzing fetal heart data.

1) HARDWARE SYSTEM

As the primary part of the hardware system, ultrasonic excitation and acquisition circuit play an essential role in our FHR detection apparatus. It mainly includes ultrasonic excitation section generation and ultrasonic echo acquisition section. The circuit schematic diagram is shown in Fig. 7. Firstly, DRIVE_A signal and DRIVE_B signal are used to control two buffers to generate a rectangular pulse signal with a phase difference of 180°. Two single-sided signals are synthesized into a positive and negative alternating excitation signal by a common-mode inductor after driving signal amplification and impedance matching. Then the resulting excitation signal is generated and used to stimulate the ultrasonic transducer. Subsequently, the ultrasonic echo signal can be detected and output from the RF_OUT pin. After that, ultrasonic echo signal amplification, band-pass filtering, and analog-to-digital conversion are performed separately on the echo signal. Finally, the processed echo signal is sent to the CPLD digital signal processing unit. In the above process, SN74LVC1G125 is employed as the buffer chip, SGM8652XS is used to amplify two-way single side signals, and SGM8654XS is utilized to convert into a single-ended signal and carried out a 980~1020 kHz band-pass filtering.

In addition, we selected 10 bit ADS825E as the ADC acquisition chip and set the A/D conversion sampling rate to 20 MSPs. To meet the requirement of a single power supply, we made the peak-peak value of the echo wave clamped to
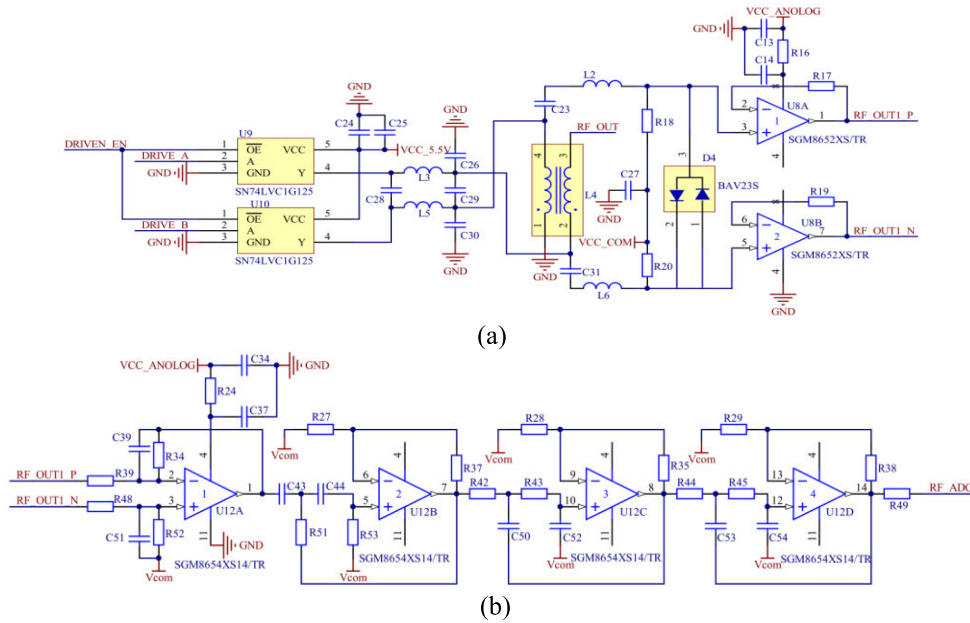
(a)

(b)

FIGURE 7. Schematic diagram of ultrasonic excitation signal generation and ultrasonic echo acquisition circuits.
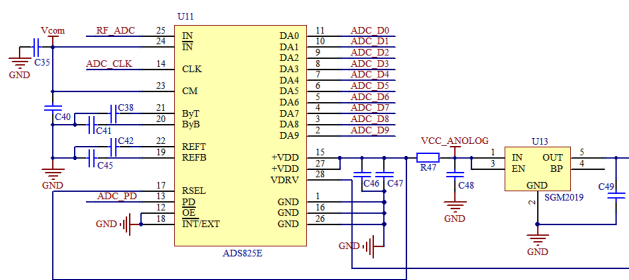

FIGURE 8. Schematic diagram of ADC acquisition circuit.

3.3 V and set the baseline to 1.65 V. The schematic diagram of the ADC acquisition circuit is shown in Fig. 8.

Moreover, the CPLD digital signal processing is based on the EPM570T100C5N chip in our FHR detection system. After the analog-to-digital conversion, to eliminate the interference caused by power supply noise, a digital high-pass filter is carried out on the echo data. Also, we use an optimized infinite impulse response (IIR) filter to realize high-pass filtering. The expression is

$$y(n) = \frac{57}{64}[x(n) - x(n-1) + y(n-1)] \qquad (11)$$

Besides, the −1dB cut-off frequency of the IIR high-pass filter is set to 750 kHz. Due to the limited hardware logic resources of the CPLD chip, it is not easy to carry out division operations. Therefore, firstly, we adopt the shifting method and then accumulate data to realize IIR filtering. Since the above method does not need multiplication and division operations, the digital filtering process can save many hardware logic resources for digital demodulation. The flow diagram of the IIR high-pass filter is shown in Fig. 9.

According to the algorithm flow diagram shown in Fig. 5, firstly, the ultrasonic echo data is windowed with the in-phase window function and the orthogonal window function to obtain the windowed sequence of I signal and the windowed sequence of Q signal. Then the accumulation operation is carried out, and then the velocity of fetal heart movement is derived according to Eq. (10). Finally, the fetal heart's velocity curve and the FHR are obtained.

Additionally, the original data such as the fetal heart movement's instantaneous direction, instantaneous FHR, average FHR, the detection depth, and fetal heart curve are derived and sent to MCU through SPI bus line for parsing, flash storage, OLED display. The MCU is connected with a WiFi module through a serial port to transmit the fetal heart data to the UC. The FHR, trend curve of FHR and status information can be real-time dynamically displayed by the UC equipped with corresponding software. Simultaneously, the OLED screen on the wireless FHR detector displays the remaining battery power, the connection status, the working status of the detection system, and other information. Besides, our proposed wireless FHR detection system can also have the functions such as charge the lithium battery through a USB interface, charge and discharge management of the battery.

2) SOFTWARE SYSTEM

The STM32F103RCT6 is used as the primary control processor in software design and developed on the Keil MDK 5.11 platform. It automatically searches for a wireless local area network (LAN) hotspot to perform configuration after turning on the wireless FHR detector. The UC's routing hotspot is used to configure the corresponding
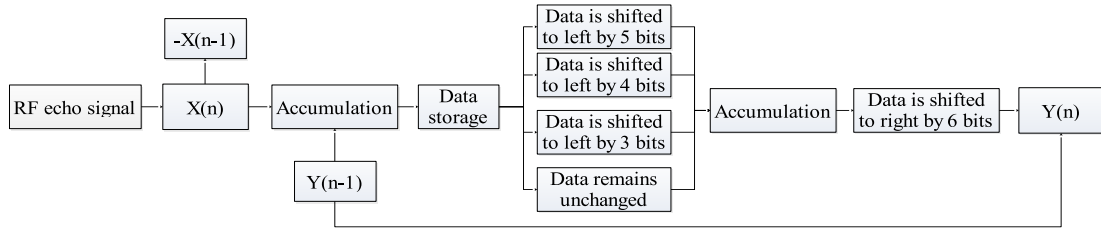
FIGURE 9. Flow diagram of IIR high-pass filter.

WiFi parameters. When the FHR detector's WiFi finds the routing hotspot, the program enters the WiFi configuration state. After finishing the WiFi configuration, it enters the normal WiFi connection process. According to the MCU internal flash memory data, the FHR detector's MCU automatically connects to the UC's wireless LAN hotspot.

After the WiFi was connected successfully, the MCU automatically generates the serial number according to the UC's IP address. According to the serial number, the user can select the corresponding FHR detector to perform the startup operation. The wireless FHR detector then realizes the related functions according to the commands sent by the UC. Finally, the wireless FHR detector transmits fetal heart data and working status information to the UC. The software flowchart of the wireless FHR detector is shown in Fig. 10.

In our software design, the serial number aims to identify the UC and the wireless FHR detector's identification in the above process. The UC is used to receive and process the data of the available wireless FHR detectors. If an individual wireless FHR detector detects the FHR exceeds the threshold value, or the working state is abnormal, it will automatically send a warning by flashing screen and a warning sound to inform the abnormals.

3) DESIGN OF THE ULTRASONIC TRANSDUCER

As the ultrasonic Doppler fetal heart signal is a non-stationary signal, maternal respiration, maternal heartbeat, blood flow, and other factors easily interfere with it. Additionally, the fetal heart movement in the maternal abdomen is small. Thus it is difficult to accurately collect weak fetal heart signals from the pregnant woman exposed to various noise interference environments [28]. Moreover, it is hard to accurately estimate the position of the fetal heart. Thus it is difficult to accurately and stably receive the FHR. To increase the measurement area and improve the detection sensitivity, we design a circular transducer composed of nine single element probes and used as the excitation and detection transducer. The center frequencies of the nine single element probes are 1 MHz.

To clearly distinguish fetal heartbeat and improve the FHR identification rate, we increased the ultrasonic emission power and improved the detector's signal-to-noise ratio (SNR). We added an impedance matching circuit between the ultrasonic transducer and the driving signal amplification to
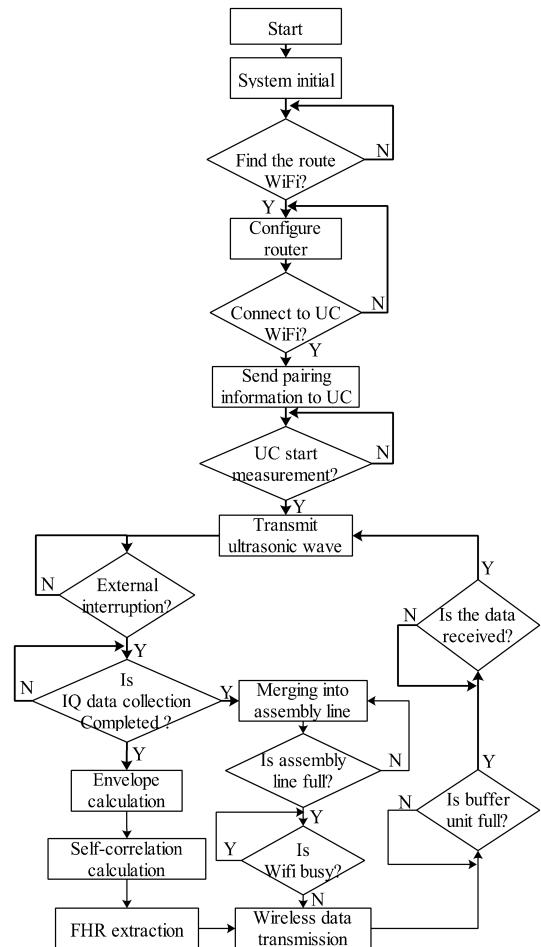

FIGURE 10. The software flowchart of the wireless FHR detector.

obtain the maximum emission power. To expand the ultrasonic acoustic radiation area and increase fetal heart position accuracy, we arranged nine ultrasonic piezoelectric ceramic probes in a "plum blossom" shape, and the probes are connected in parallel. The transducer's internal structure, the circuit board of the wireless FHR detector, and the physical diagram are shown in Fig. 11.

B. REALIZATION OF TIME-DOMAIN WINDOWED DIGITAL FHR DEMODULATION ALGORITHM

According to the time-domain windowed digital FHR demodulation process's block diagram shown in Fig. 4.
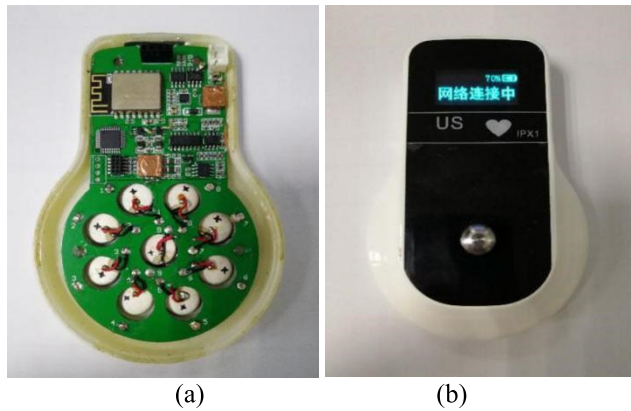
FIGURE 11. Practicality diagram: (a) the circuit board of the proposed FHR detector. (b) The front view.

FIGURE 12. Structure frame of multi-FHR monitoring system.

Our proposed digital FHR demodulation algorithm only needs a multiplier and two adders. It largely reduces the logical hardware resources and it is different from the traditional digital FHR demodulation algorithm. In our digital FHR demodulation, the demodulation window function sequence of the I signal can be set as

$$Z^I = \{z^I(1), z^I(3), z^I(4), z^I(5)...z^I(n)\}$$

Supposing that the demodulation window function sequence of Q signal is written as

$$Z^Q = \{z^Q(1), z^Q(3), z^Q(4), z^Q(5)...z^Q(n)\}$$

Then the time-domain windowed digital FHR demodulation process can be expressed as below:

(a) Firstly, the echo signal $x(1)$ and $z^I(1)$ are sent into the multiplier.

(b) Then, adder_I opens, adder_Q is turned off, and then the data from the multiplier are added to the data in the Y1 register.

(c) Subsequently, $x(1)$ remains unchanged, and $z^Q(1)$ is fed into the multiplier.

(d) After that, adder_Q opens, adder_I is turned off, and the data from the multiplier are added to the data in the Y2 register.

(e) Next, the echo data $x(3)$, and $z^I(3)$ are sent into the multiplier.

(f) Then, adder_I opens, and adder_Q is turned off, and then the data from the multiplier are added to the data in the Y1 register.

(g) In the same way, $x(3)$ remains unchanged, and $z^Q(3)$ is fed into the multiplier.

(h) Then, adder_Q opens, adder_I is turned off, and the data from the multiplier are added to the data in the Y2 register.

(i) Next, loop in the data as before, and the calculation is repeated according to the previous method. Until all the ultrasonic echo data and window function sequence are sent to the operation, the I signals and the Q signals are obtained. Finally, the IQ signal is sent to MCU for further processing. The above are the primary processes of time-domain windowed digital
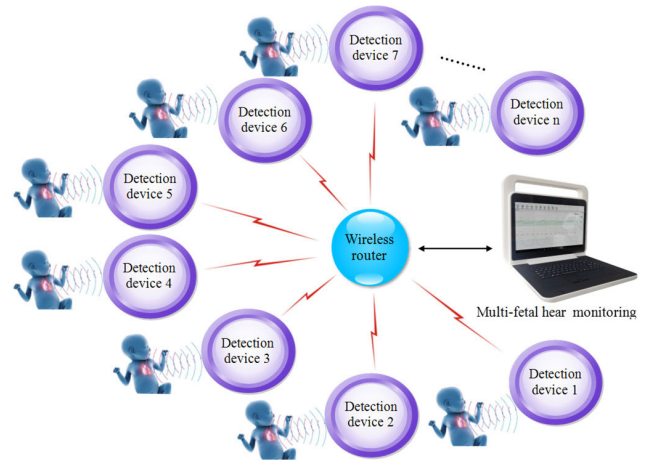
FHR demodulation of single ultrasonic echo data in a pulse repetition period.

Compared with the traditional digital FHR detector, the time-domain windowed FHR digital demodulation algorithm omits the redundant multi-stage multiplier and reduces the CPLD chip's hardware logic resources. It is possible to realize the same function of the traditional digital FHR demodulation algorithm, and it can be applied to a low price, low-power consumption CPLD chip.

C. REALIZATION OF MULTI-FHR MONITORING SYSTEM

To improve monitoring efficiency, reduce FHR monitoring costs, and provide abnormal FHR alarms in various healthcare settings. We developed and implemented a prototype multi-FHR monitoring system. A WiFi modular is employed to connect the multi-FHR monitoring host with the FHR detectors to transmit and display the fetal heart data. As the central data analysis, monitoring, and display terminal, the multi-FHR monitoring host provides a wireless local area network to wireless FHR detectors to access, controls the wireless FHR detector and collects FHR monitoring data from the wireless FHR detectors, and finally realizes multiple data processing, display, and warning functions. As an application part, the wireless FHR detector can be freely connected to the local area network of the multi-FHR monitoring host and can accurately detect FHR. Finally, the compressed and encoded fetal heart data are sent to the monitoring host. The whole architecture of the multi-FHR monitoring system is shown in Fig. 12.

Additionally, in this work, a power module named RPS-160-12 is utilized to suffer power for the multi-FHR monitoring host, which can be treated as a UC. An RK3399 is used as the multi-FHR monitoring host processor, and a 17.3 inch OLED screen is adopted as the display module of FHR data and working status. Besides, the built-in wireless router module of the multi-FHR monitoring host is used to build a wireless LAN to access available wireless FHR detectors, and the wireless router module can provide 32 IP

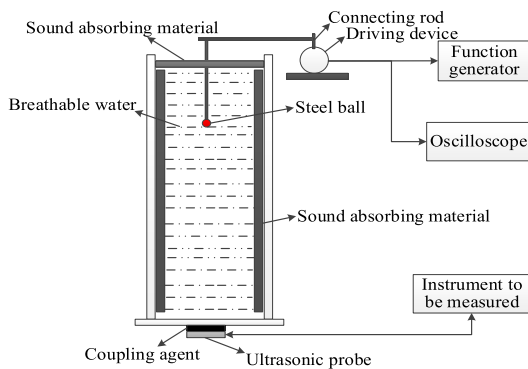**FIGURE 13.** Appearance of our multi-FHR monitoring host.

FIGURE 14. Schematic diagram of the FS-3 FHR simulator.

addresses, which can be assigned to the external available wireless FHR detectors. After the multi-FHR monitoring host is powered on, it receives the available wireless FHR detectors' access requests in real-time. The monitoring host excludes other non-system defined hardware devices according to the wireless FHR detectors' handshake signal. Therefore, that ensures all the defined wireless FHR detectors match with the multi-FHR monitoring host. The appearance of our multi-FHR monitoring host is shown in Fig. 13.

IV. EXPERIMENTS

A. PERFORMANCE AND ACCURACY EVALUATION OF OUR WIRELESS FHR DETECTION SYSTEM

As the fetal heart movement's beating action can be imitated through the steel ball's up and down motion, the steel ball's motion amplitude can be adjusted to imitate different fetal heart curves' heartbeat amplitude. Therefore, we selected the comprehensive sensitivity test simulator (FS-3, the institute of acoustics, the Chinese Academy of Sciences, Beijing, China) as the imitation target of fetal heart movement to generate FHR test curves. As the FS-3 FHR simulator's steel ball is connected with a function generator through a driving device and a connecting rod, which can generate several classical FHR curves. Therefore, we can control the FS-3 FHR simulator's steel ball movement to imitate different fetal heart movements by selecting different FHR test curves. The FS-3 FHR simulator's composition structure is shown in Fig. 14.

In our accuracy evaluation experiments, the ultrasonic transducer was placed close to the sound window at the lower end of the FS-3 FHR simulator. The ultrasonic coupling agent was applied between the ultrasound probe and the sound window of the FS-3 FHR simulator. Then, the ultrasonic probe emitted the ultrasonic beam through the sound window, and then the ultrasonic beam was reflected by the steel ball in motion. After receiving the ultrasonic echo signal, the FHR curve and FHR value were obtained by processing the subsequent echo signal.

As the TREND curve had significant amplitude variation and a relatively wide dynamic FHR range, it rapidly changed from 90 to 160 BPM. Thus, the dramatic FHR variation could effectively test the detection system's accuracy in an extensive amplitude range. Therefore, we adopted the TREND curve built-in in the FS-3 simulator to carry out comparative analysis in this experiment. The test time on our wireless FHR detector was set to 20 minutes. After the experiment, the fetal heart monitoring records in Excel format were derived from the multi-FHR monitoring host. Then, the wireless FHR detector's monitoring curve was generated from the recorded data, and then the accuracy comparison curves in the TREND curve mode were derived, which was shown in Fig. 15.
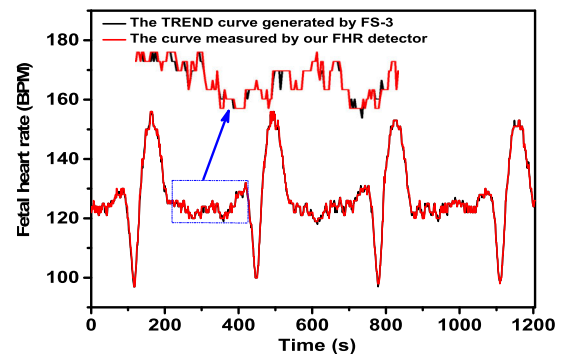

FIGURE 15. Comparison curve in TREND curve mode.

B. FHR DOUBLING PERFORMANCE TESTING

The FHR doubling is a false recognition that the measured FHR is twice the actual FHR in clinical practice. The primary reason for FHR doubling is that there is a time interval between the positive and negative movement of the mitral valve in a systolic-diastolic cycle, leading to the recognition of two Doppler shifts in one cycle. With its inability to distinguish the direction of fetal heart movement, the traditional analog demodulation FHR detection instrument often identifies a positive and negative movement of the mitral valve as two heartbeats, which easily results in the wrong FHR recognition. To prevent the FHR doubling, we proposed a digital demodulation algorithm based on time-domain windowing and adopted a low-cost and low-power CPLD chip to perform digital FHR demodulation for achieving low-cost and accurate acquisition of vector velocity of fetal heart movement.

TABLE 1. Accuracy analysis of our wireless FHR detector.

Simulator(BPM)	FM-3A(BPM)	Accuracy	σ_1(BPM)	Our system(BPM)	Accuracy	σ_2(BPM)
60	127	47.20 %	3.03	61	98.40%	1.41
80	151	52.98%	2.32	79	98.75%	1.09
100	176	56.80%	1.79	100	100.00 %	0.77
120	117	97.50%	1.09	121	99.17%	0.54
140	141	99.30%	0.89	140	100.00%	0.45
160	158	98.70%	1.18	162	98.80%	0.83
180	178	98.88 %	1.26	179	99.44 %	0.89
200	200	100.00 %	1.41	201	99.50%	1.26
Average	-----	81.42%	1.62	-----	99.25%	0.91

Additionally, to further test our method's validation metrics, we conducted the same experiment on the commercial FM-3A FHR detector by the same method above for verifying our designed FHR detector's accuracy and reliability. The FHR test curves generated by the FS-3 FHR simulation were used to test our proposed digital FHR detector's performance. A ten-minute comparative experiment between the commercial FM-3A FHR detector and our proposed FHR detector was carried out in our study. In this verification experiment, firstly, the test FHRs of 60, 80, 100, 120, 140, 160, 180, and 200 BPM were produced by the FS-3 FHR simulator. Then, the generated FHR were measured simultaneously by our FHR detector and a commercial FM-3A FHR detector (traditional analog demodulation FHR device) manufactured by Shenzhen Airuikang Medical Equipment Co., Ltd in China for 10 minutes. The FHR data was collected every minute, and a total of 10 FHR values were obtained in 10 minutes. Subsequently, the average value of 10 FHRs of the two sets of devices in 10 minutes was calculated respectively. Finally, our wireless FHR detector's relative error and standard error were analyzed by the performance comparison between the commercial FM-3A detector and our designed FHR detector. The accuracy analysis of our wireless FHR detector and the two FHR apparatus's experimental results are shown in Table 1.

To further demonstrate our designed wireless FHR detector can inhibit the FHR doubling and clarify the reasons resulting in the FHR detection difference, we set the FS-3 FHR simulator to generate an FHR signal with 75 BPM by manually pressing the function button. Then, the FM-3A FHR detector and our designed FHR detector were used to detect the test FHR, and then a digital oscilloscope (MD03052, Tektronics Inc., USA) was used to intercept the Doppler frequency shift signal of the FM-3A detector and the velocity curve of our proposed FHR detector. In the above process, the Doppler frequency shift signal of the FM-3A detector was introduced from the audio signal line, the Doppler FHR curve detected by the FM-3A detector was indistinctly shown in Fig. 16 (a). Our designed wireless FHR detector's velocity curve comes from the DAC pin of the STM32F103RCT6 microprocessor, and the vector velocity curve detected by our proposed FHR detector was clearly shown in Fig. 16 (b). Finally, a performance comparison between the FM-3A FHR detector and

(a)

(b)
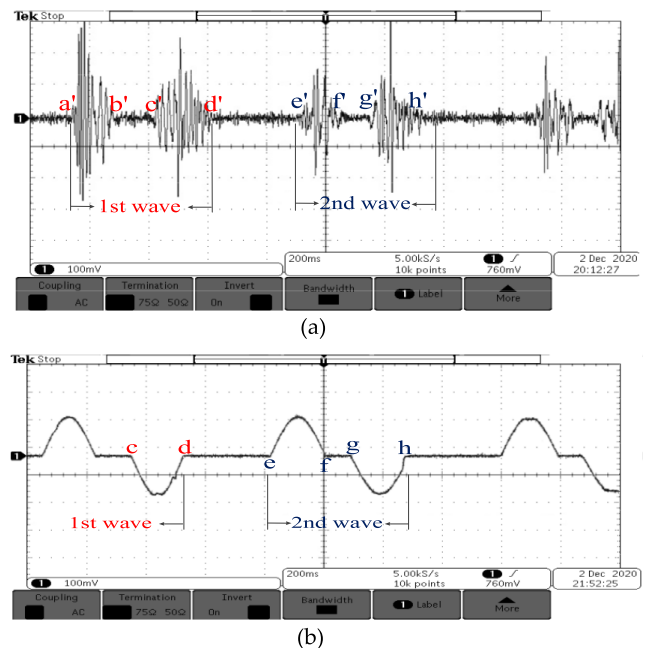
FIGURE 16. Performance comparison between FM-3A FHR detector and our designed FHR detector. (a) FHR curve detected by FM-3A FHR detector. (b) Vector velocity curve detected by our FHR detector.

our designed FHR detector is carried out to demonstrate that our proposed FHR detector can easily distinguish a fetal heartbeat's positive and negative directions and effectively overcome FHR doubling.

To further test the detection performance, we performed a five-minute FHR measurement experiment in real conditions. Before the measurement, a 28-year-old pregnant woman with normal single pregnancy at the gestational age of 30 weeks was in a quiet resting state for 20 minutes, and then the FHR measurement experiment was performed on the pregnant woman by our proposed digital FHR detector using time-domain windowing. It presented that the five-minute FHR monitoring curve was from 130 to 135 BPM, and it proved the stability of our proposed FHR detection system.

Moreover, we adopted the Verilog hardware description language as the programming language to program the

unoptimized/optimized FHR digital demodulation algorithm through the EDA software (Quarrtes II). In the FHR demodulation part, the FHR detection algorithm was optimized by using time-domain windowed digital demodulation. The CPLD hardware resources required for code execution were 4% of the hardware resources needed before optimizing the digital demodulation algorithm. i.e., the Quartus II software calculated the reduction in computation. As our proposed FHR detection algorithm using time-domain windowed digital demodulation dramatically reduced the hardware resources required for FHR digital demodulation, the proposed FHR detection algorithm could run on a lower-cost CPLD chip, reducing the cost and volume of the traditional digital demodulation FHR detector.

V. RESULTS
In our study, an accuracy verification comparison between the TREND curve generated by the FS-3 FHR simulator and the curve measured by our proposed FHR detector was carried out. Two comparison curves of accuracy are presented in Fig. 15, which shows that the two FHR curves' trends and amplitude changes are almost identical. Besides, our wireless FHR detector's average error within the test range does not exceed ±1 BPM(actually about ± 0.9 BPM), which indicates that our proposed wireless FHR detector has high accuracy in terms of FHR measurement. Although some errors exist between the TREND curve generated by the FS-3 FHR simulation and the curve measured by our proposed FHR detector, the average error range is not more than ±1 BPM. According to the Chinese national standard on hand-held probe Doppler FHR detector and measurement method (YY/T 0749-2009/IEC 61266:1994), the average error of FHR measurement should not exceed ±2 BPM, which means the FHR measured by our wireless FHR detection system is within the error range. Besides, our designed wireless FHR detector can work continuously for more than 10 hours, which shows that our proposed digital demodulation algorithm reduced the FHR computation amount and indicates applying the digital FHR demodulation algorithm to the low-power CPLD chip is practical and feasible.

As shown in Table 1, when the FS-3 FHR simulator's output is set as 60, 80, and 100 BPM, the average value of 10 FHRs measured by the commercial traditional analog demodulation Doppler FHR detector (FM-3A) in 10 minutes is 127, 151, and 176 BPM, respectively. The measured average values by FM-3A are almost twice the actual values, which means that FHR doubling occurs. It indicates that the commercial FM-3A detector cannot suppress the FHR doubling. As the commercial FM-3A detector uses an analog demodulation method that only extracts the I signal or the Q signal from the ultrasonic echo signals. It theoretically cannot suppress the FHR doubling and cannot obtain the fetal heart's motion direction. Therefore, the possible reasons for the error in estimating 60, 80, and 100 BPM seem that the commercial FM-3A detector occurs obvious FHR doubling in detecting 60, 80, and 100 BPM. Sometimes the FHR doubling

is detected, and sometimes the original FHR is detected. Therefore, the average value of the detected FHR is greater than the original FHR and is less than twice the actual FHR. Besides, while the average value of 10 FHRs measured by our designed wireless FHR detector is 61, 79, and 100 BPM, it indicates that the detection accuracy of our detection system is much higher than that of the FM-3A detector when the test FHRs are 60, 80, and 100 BPM. When the FS-3 FHR simulator's output is set as 60, 80, 100, 120, 140, 160, 180, and 200 BPM, our proposed digital demodulation FHR detector's accuracy is higher than that of the commercial FM-3A detector. When the test FHRs are 120, 140, and 160 BPM, our proposed digital demodulation FHR detector's average accuracy is around 99%, which is slightly higher than that of the commercial equipment. When the test FHRs are 120, 160, 180, and 200 BPM, the average accuracy of the proposed digital demodulation FHR detector is equivalent to that of the commercial FM-3A detector. It means that both the two apparatuses can accurately detect the FHR in detecting 120, 160, 180, and 200 BPM. As a time-domain windowed digital FHR demodulation algorithm is applied in our wireless FHR detector, the fetal heart movement's obtained velocity is a vector. Therefore, the wireless FHR detection system based on time-domain windowing shows good inhibition ability of FHR doubling. Its average accuracy rate of FHR reaches 98%, which is much higher than the average accuracy (81%) of the FM-3A detector. The relative error and standard error of the obtained FHR data are used to analyze and evaluate the two FHR detectors' detection accuracy. The result shows that our designed FHR fetal heart rate detector's average error is slightly lower than the commercial FM-3A FHR detector (actually about ±1.6 BPM). The above experiments demonstrate that the wireless FHR detector designed in this paper has high detection accuracy and can meet the Chinese national standard of ultrasonic Doppler FHR monitor and modern medicine requirements for FHR detection accuracy.

Moreover, a performance comparison between the FM-3A FHR detector and our designed FHR detector is carried out to demonstrate our proposed FHR detector can easily distinguish a fetal heartbeat's positive and negative directions and effectively overcome FHR doubling, which is shown in Fig. 16. As shown in Fig.16(a), five pulse waves with different amplitudes and time widths are presented. It is difficult to distinguish the steel ball's rising and falling time and identify the differences in phase and amplitude when the steel ball is rising or falling. The related experiment demonstrated that the FM-3A detector might misjudge a round-trip movement of the steel ball as two fetal heart movements at certain times, reflecting that the traditional analog demodulation Doppler FHR detector easily leads to the FHR doubling. However, in our proposed FHR detection system, a vector velocity is obtained by IQ digital demodulation, which can be applied to distinguish FHR. As shown in Fig.16(b), a~b and c~d represent the falling and rising process of the steel ball, respectively, and e~f and g~h denote the falling and rising movements of the next beating. The fetal heart's rise and fall

direction are apparent, the amplitude of the velocity curve detected by our FHR detector is stable. The positive and negative changes in the velocity curve during a round-trip movement of the steel ball can clearly show the steel ball's rising and falling processes in a single motion. Therefore, a fetal heartbeat's positive and negative directions can be clearly distinguished in our FHR calculation. It indicates that our proposed FHR detector can effectively overcome FHR doubling, and more accurate FHR values can be obtained.

In conclusion, the above experiments demonstrate that the proposed digital demodulation FHR detector based on time-domain windowing is accurate and feasible and can effectively overcome FHR doubling. The proposed wireless FHR detector has met the requirements of the Chinese national standard and obtained the medical device registration certificate (NO. 20192180323) in 2019. Therefore, it is qualified for medical applications, can offer comparable performance to the commercial FHR detector, and is expected to be widely used in future FHR detection.

VI. DISCUSSION

The digital demodulation FHR detectors, which have hand-held characteristics, low-power consumption, and low-cost and can obtain accurate FHR, are rarely reported. So it is important to investigate the new FHR evaluation technology. Although the traditional analog FHR demodulation method has the advantages of low-power consumption, low cost, small size, affordable hand-held, and ease to carry, the fetal heart movement's vector velocity cannot be obtained and easily cause the FHR doubling. While the traditional digital FHR demodulation method can obtain the fetal heart movement's vector velocity, which indicated it could inhibit the FHR doubling and show the mean time interval of each of the cardiac events. However, it is large in size, non-handheld, high in power consumption, expensive in cost, and redundant in functions. Therefore, a novel digital FHR demodulation algorithm based on time-domain windowing was proposed, a portable wireless ultrasonic Doppler detector using the demodulation algorithm was designed and implemented, and a prototype multi-FHR monitoring system was built. It was different from the existing FHR detection methods that generally use offline processing methods and different optimization algorithms to simultaneously process 1-DUS signal/fECG data for jointly improving the accuracy of FHR estimation. It was also different from the traditional analog demodulation FHR detection methods that only extract the I signal or Q signal from the ultrasonic echo signals. This work aims to develop a new multi-FHR digital demodulation monitor and realize low-cost, low-power FHR detection, which can be used for simultaneous monitoring of multiple FHR, identify the fetal heart movement's direction, and be used for accurate FHR detection with low cost and low power consumption.

In this work, to effectively reduce the heat dissipation and power consumption and conserve the battery life for the wireless FHR detector, a low-cost and low-power CPLD chip with a limited hardware logic resource was utilized to realize digital FHR demodulation. A circular transducer composed of nine single element probes was applied as the excitation and detection transducer to enhance the FHR detection sensitivity of our proposed Doppler FHR detector. Moreover, the FHR vector kinematics parameters' acquisition and analysis were realized by our proposed demodulation method. We also adopted modular design method to improve monitoring efficiency and reduce FHR monitoring costs in this work. For instance, the multi-FHR monitoring host and wireless FHR detector were connected by WiFi. It could simultaneously monitor multiple pregnant women's FHR. The multi-FHR monitoring host's monitoring interface was user-friendly, easy to operate, high monitoring efficiency, non-invasive and radiation-free, and could be applied in hospitals, communities, homes, and other environments. It also could be used for multiple pregnant women to use at any time.

Meanwhile, in our accuracy evaluation experiments, an accuracy verification comparison between the TREND curve generated by the FS-3 FHR simulator and the curve measured by our proposed FHR detector was carried out. As shown in Fig. 15, the trends and amplitude changes of the two FHR curves were almost identical, and our wireless FHR detector's average error within the test range did not exceed ± 1 BPM. It implied that the proposed wireless FHR detector has met the requirements of the Chinese national standard and is qualified for medical applications. Additionally, we conducted the same experiment on the commercial FM-3A FHR detector by the same method. It showed that the average accuracy of FM-3A within the test range did not exceed ± 2 BPM, which demonstrated that the FM-3A FHR detector also met the national standard. Moreover, the relative error and standard error of the obtained FHR data are used to analyze and evaluate the two FHR detectors' detection accuracy.

As shown in Table 1, the measured average values by FM-3A were almost twice the actual values when the FS-3 FHR simulator's output was set as 60, 80, and 100 BPM. It indicated that the commercial FM-3A detector cannot suppress the FHR doubling and occur obvious FHR doubling in detecting 60, 80, and 100 BPM. It also demonstrated that our detection system could effectively prevent the FHR doubling and the detection accuracy of our detection system was much higher than that of the FM-3A detector when the test FHRs were 60, 80, and 100 BPM. The relative measurement errors and analysis comparing the FHR estimation results have been analyzed and evaluated. The results revealed that the wireless FHR detection system based on time-domain windowing showed good inhibition ability of FHR doubling and was much higher than the average accuracy of the FM-3A detector, and its average error was slightly lower than the commercial FM-3A FHR detector.

As shown in Fig. 16, the performance comparison between the FM-3A FHR detector and our designed FHR detector was presented in our study. It demonstrated that our proposed FHR detector could easily distinguish a fetal heartbeat's positive and negative directions and effectively overcome

FHR doubling. As our proposed FHR detection algorithm using time-domain windowed digital demodulation dramatically reduced the hardware resources required for FHR digital demodulation, the proposed FHR detection algorithm could run on a lower-cost CPLD chip, which reduced the cost and volume of the traditional digital demodulation FHR detector.

Since most of the existing FHR estimations used the public data sets for analysis and further digital signal processing on 1-DUS signals, the accuracy analysis of FHR estimations usually used fECG for reference. However, in our study, it was not easy to obtain synchronized fECG data. Therefore, relative error analyses and standard error analyses were carried out in our manuscript. Further digital signal processing of 1-DUS signals and quantitative error and statistical analysis with other commercial instruments will be the focus of our subsequent work. Although the digital logic resource needed in our proposed digital FHR demodulation algorithm was only about 4% of the traditional digital FHR demodulation algorithms, it was not verified by real data. Although the comparative experiments proved that our proposed digital Doppler FHR detection system could achieve a high detection accuracy than the commercial FM-3A FHR detector, our proposed FHR detection system was not tested on a large scale. Therefore, our next focus is to expand the analysis to cover many samples on both normal and abnormal FHR Doppler signal samples. It is also necessary to conduct relevant experiments to track and measure pregnant women with different pregnancy cycles for verifying the accuracy and applicability of the wireless digital FHR detection system. It will be the emphasis of our subsequent study.

VII. CONCLUSION

In our work, the TREND test curve was generated by the FS-3 FHR simulation, the comparison curve between the TREND curve generated by the FS-3 FHR simulation and the measured curve of our proposed FHR detector was obtained. A comparative experiment between the commercial FM-3A FHR detector and our proposed FHR detector was carried out. The FS-3 FHR simulator produces eight test FHRs, and the generated FHRs were measured by our FHR detector and the commercial FM-3A FHR detector. Then, the relative error and standard error of the obtained FHR data were used to analyze and evaluate two FHR detectors' detection accuracy, and the detailed comparison in heart rate estimation was investigated. Subsequently, a performance comparison between the FM-3A FHR detector and our designed FHR detector was carried out. The results show that the detection accuracy of the FM-3A FHR detector is low, and it easily leads to FHR doubling due to it calculated the FHR based on the single-channel analog demodulation signal. However, our proposed digital FHR demodulation algorithm easily distinguished a fetal heartbeat's positive and negative directions, effectively overcome FHR doubling defects, and meet Chinese national standards' requirements.

The detection accuracy rate of our designed FHR detector reached 98%, which was much higher than the average accuracy of FM-3A and indicated that our proposed digital FHR detector showed excellent detection performance. It also presented that our designed FHR detection system had a broad application prospect because of its portability, accuracy, digitization, high-cost performance, and adjustable detection depth. It will provide an alternative scheme towards the low-cost hand-held digital demodulation FHR detection application and is of great significance to improve fetal separation quality, reduce fetal mortality, inhibit the birth of congenital disabilities and mentally retarded fetuses.

COMPETING INTERESTS
The authors declare no conflict of interest.

REFERENCES

[1] M. F. Macdorman and E. C. W. Gregory, "Fetal and perinatal mortality: United States, 2013," *Nat. Vital Statist. Rep.*, vol. 64, no. 8, pp. 1–23, 2015.

[2] X. Hua, L. Kaiqing, and Z. Zhenxi, "A new algorithm for detecting fetal heart rate using ultrasound Doppler signals," *Ultrasonics*, vol. 43, no. 6, pp. 399–403, May 2005.

[3] B. Karlsson, M. Berson, T. Helgason, R. T. Geirsson, and L. Pourcelot, "Effects of fetal and maternal breathing on the ultrasonic Doppler signal due to fetal heart movement," *Eur. J. Ultrasound*, vol. 11, no. 1, pp. 47–52, Mar. 2000.

[4] P. V. S. Stephanie, A. L. Boulesteix, C. Lederer, S. Grunow, S. Schiermeier, W. Hatzmann, K. T. M. Schneider, and M. Daumer, "What is the 'normal' fetal heart rate?" *Peerj*, vol. 12, p. e82, Jan. 2013.

[5] B. J. Trudinger, C. M. Cook, L. Jones, and W. B. Giles, "A comparison of fetal heart rate monitoring and umbilical artery waveforms in the recognition of fetal compromise," *BJOG, Int. J. Obstetrics Gynaecol.*, vol. 93, no. 2, pp. 171–175, Feb. 1986.

[6] P. Chetlur Adithya, R. Sankar, W. A. Moreno, and S. Hart, "Trends in fetal monitoring through phonocardiography: Challenges and future directions," *Biomed. Signal Process. Control*, vol. 33, pp. 289–305, Mar. 2017.

[7] E. H. Hon, "The electronic evaluation of the fetal heart rate," *Obstetrical Gynecol. Surv.*, vol. 13, pp. 654–656, Oct. 1958.

[8] R. C. Goodlin, "History of fetal monitoring," *Amer. J. Obstetrics Gynecol.*, vol. 133, no. 3, pp. 323–352, Feb. 1979.

[9] K. Hammacher, "New method for the selective registration of the fetal heart beat," *Geburtshilfe Frauenheilkunde* vol. 22, pp. 1542–1543, Dec. 1962.

[10] J. Y. Kwon and I. Y. Park, "Fetal heart rate monitoring: From Doppler to computerized analysis," *Obstetrics Gynecol. Sci.*, vol. 59, no. 2, p. 79, 2016.

[11] P. A. Warrick, E. F. Hamilton, R. E. Kearney, and D. Precup, "A machine learning approach to the detection of fetal hypoxia during labor and delivery," *AI Mag.*, vol. 33, no. 2, p. 79, Mar. 2012.

[12] V. Chudacek, J. Spilka, L. Lhotska, P. Janku, M. Koucky, M. Huptych, and M. Bursa, "Assessment of features for automatic CTG analysis based on expert annotation," in *Proc. Annu. Int. Conf. IEEE Eng. Med. Biol. Soc.*, Aug. 2011, pp. 6051–6054.

[13] I. Kiefer-Schmidt, M. Lim, A. Wacker-Gußmann, E. Ortiz, H. Abele, K. O. Kagan, R. Kaulitz, D. Wallwiener, and H. Preissl, "Fetal magnetocardiography (FMCG): Moving forward in the establishment of clinical reference data by advanced biomagnetic instrumentation and analysis," *J. Perinatal Med.*, vol. 40, no. 3, pp. 277–286, Jan. 2012.

[14] K. Beng Gan, E. Zahedi, and M. A. M. Ali, "Transabdominal fetal heart rate detection using NIR photopleythysmography: Instrumentation and clinical results," *IEEE Trans. Biomed. Eng.*, vol. 56, no. 8, pp. 2075–2082, Aug. 2009.

[15] C. Zhang, S. Zhang, and S. Gao, "An improved auto-correlation method for Doppler fetal heart rate measurement," *J. Biomed. Eng.*, vol. 18, no. 3, p. 434, 2001.

[16] P. Hamelmann, R. Vullings, A. F. Kolen, J. W. M. Bergmans, and M. Mischi, "Doppler ultrasound technology for fetal heart rate monitoring: A review," *IEEE Trans. Ultrason., Ferroelectr., Freq. Control*, vol. 67, no. 2, pp. 226–238, Feb. 2019.

[17] S. Breukelman, E. J. H. Mulder, R. V. Oord, H. Jonker, B. C. van der Weijden, and M. A. M. Taverne, "Continuous fetal heart rate monitoring during late gestation in cattle by means of Doppler ultrasonography: Reference values obtained by computer-assisted analysis," *Theriogenology*, vol. 65, no. 3, pp. 486–498, Feb. 2006.

[18] A. Mert, M. Sezdi, and A. Akan, "A test and simulation device for Doppler-based fetal heart rate monitoring," *Turkish J. Electr. Eng. Comput. Sci.*, vol. 23, pp. 1187–1194, 2015.

[19] C. E. Valderrama, L. Stroux, N. Katebi, E. Paljug, R. Hall-Clifford, P. Rohloff, F. Marzbanrad, and G. D. Clifford, "An open source autocorrelation-based method for fetal heart rate estimation from one-dimensional Doppler ultrasound," *Physiol. Meas.*, vol. 40, no. 2, Feb. 2019, Art. no. 025005.

[20] S. A. Alnuaimi, S. Jimaa, and A. H. Khandoker, "Fetal cardiac Doppler signal processing techniques: Challenges and future research directions," *Frontiers Bioeng. Biotechnol.*, vol. 5, pp. 1–8, Dec. 2017.

[21] S. Alnuaimi, S. Jimaa, Y. Kimura, L. J. Hadjileontiadis, and A. H. Khandoker, "Fetal cardiac timing events estimation from Doppler ultrasound signal cepstrum analysis," in *Proc. 41st Annu. Int. Conf. IEEE Eng. Med. Biol. Soc. (EMBC)*, Jul. 2019, pp. 4677–4681.

[22] N. Katebi, F. Marzbanrad, L. Stroux, C. E. Valderrama, and G. D. Clifford, "Unsupervised hidden semi-Markov model for automatic beat onset detection in 1D Doppler ultrasound," *Physiol. Meas.*, vol. 41, no. 8, Sep. 2020, Art. no. 085007.

[23] C. H. L. Peters, E. D. M. T. Broeke, P. Andriessen, B. Vermeulen, R. C. M. Berendsen, P. F. F. Wijn, and S. G. Oei, "Beat-to-beat detection of fetal heart rate: Doppler ultrasound cardiotocography compared to direct ECG cardiotocography in time and frequency domain," *Physiol. Meas.*, vol. 25, no. 2, p. 585, 2004.

[24] A. K. Mittra, A. Shukla, and A. S. Zadgaonkar, "System simulation and comparative analysis of foetal heart sound de-noising techniques for advanced phonocardiography," *Int. J. Biomed. Eng. Technol.*, vol. 1, no. 1, pp. 73–85, 2007.

[25] P. Várady, L. Wildt, Z. Benyó, and A. Hein, "An advanced method in fetal phonocardiography," *Comput. Methods Programs Biomed.*, vol. 71, no. 3, pp. 283–296, Jul. 2003.

[26] J. R. A. Jensen, "Medical ultrasound imaging," *Prog. Biophys. Mol. Biol.*, vol. 93, pp. 153–165, Oct. 2007.

[27] C. Kasai, K. Namekawa, A. Koyano, and R. Omoto, "Real-time two-dimensional blood flow imaging using an autocorrelation technique," *IEEE Trans. Sonics Ultrason.*, vol. SU-32, no. 3, pp. 458–464, May 1985.

[28] P. Zhang, S. Ye, Z. Huang, D. Jiaerken, and J. Wu, "A noninvasive continuous fetal heart rate monitoring system for mobile healthcare based on fetal phonocardiography: Technology," *Commun. Comput.*, pp. 191–204, 2019.

KAI ZHAN received the B.S. degree in biomedical engineering from Shenzhen University, China, in 2015. He is currently the Technical Director working with JOINTO Technology Company Ltd., Changsha, China. His research interests include ultrasonic imaging and ultrasonic therapy.

RONGCHAO PENG received the bachelor's and master's degrees in biomedical engineering from the Department of Biomedical Engineering, Sun Yet-sen University, Guangzhou, China, in 2009 and 2012, respectively, and the Ph.D. degree in computer application technology from the Shenzhen Institutes of Advanced Technology, Chinese Academy of Sciences, Shenzhen, China, in 2015. His current interests include wearable medical device, digital signal processing, and computational neuroscience.

JINFENG XU received the M.D. degree in imaging medicine and nuclear medicine from Tongji Medical College, Huazhong University of Science and Technology, in 2009. He joined the Department of Ultrasonography, Shenzhen People's Hospital, as a Doctor. He was a Visiting Scholar with Oregon Health and Science University. He is currently a Chief Physician and the Director of the Department of Ultrasonography, Shenzhen People's Hospital, and a Professor and a Doctor Supervisor with The Second Clinical Medical College, Jinan University. He participated in the development of national guidelines for ultrasound diagnosis of thyroid and breast. His research interests include ultrasound diagnosis of abdominal, thyroid, breast, and peripheral vascular diseases.

HUI LUO received the M.D. degree in imaging medicine and nuclear medicine from Xiangya Medical College, Zhongnan University, in 1999. She was a Visiting Scholar with Thomas Jefferson University Hospital, Philadelphia, PA, USA, in 2018. She is currently a Chief Physician and Deputy Director of the Department of Ultrasonography, Shenzhen People's Hospital, The Second Clinical Medical College, Jinan University. Her research interests include ultrasound diagnosis of breast, thyroid, and abdominal diseases.

MING DAI received the B.S. degree in computer science and technology from Hainan Tropical Ocean University, Sanya, in 2012, the M.S. degree in electronics and communication engineering from Nanchang Hangkong University, Nanchang, and the Shenzhen Institutes of Advanced Technology, Chinese Academy of Sciences, Shenzhen, in 2015, and the Ph.D. degree in information and communication engineering from Shenzhen University, Shenzhen, in June 2019. He was a Visiting Scholar with The Chinese University of Hong Kong, from 2019 to 2020. He is currently a Postdoctoral Researcher with Jinan University and study at Shenzhen People's Hospital (The Second Clinical Medical College), Jinan University. Once his postdoctoral position is out of the station, he will soon go to Shenzhen Polytechnic as a Lecturer. His research interests include electrical conductivity imaging, biomedical multimodal data fusion, image processing, artificial intelligence, the Internet of Things engineering, big data technology and application, wearable medical applications, and design of electrical systems.

YINGYING LIU received the M.D. degree in imaging medicine and nuclear medicine from Tongji Medical College, Huazhong University of Science and Technology, in 2010. She was a Visiting Scholar with Cleveland Clinic, Cleveland, OH, USA, in 2016. She is currently an Associate Chief Physician with the Department of Ultrasonography, Shenzhen People's Hospital, and an Associate Professor and a Master Supervisor with The Second Clinical Medical College, Jinan University. Her research interests include cardiovascular ultrasound and molecular imaging.

LIANGPING LUO received the M.S. degree in imaging medicine and nuclear medicine from Jinan University, in 1991, and the Ph.D. degree from Humboldt University, Germany. He then joined the Department of Medical Imaging, The First Affiliated Hospital of Jinan University, as a Doctor. In June 2000, he was a Postdoctoral Researcher with Jinan University, and then became a Professor. He is currently a Ph.D. Tutor. His research interests include comprehensive imaging diagnosis of thoracic diseases, especially lung cancer and pleural tumors, and the study of molecular biology basis.

SIPING CHEN received the Ph.D. degree in biomedical engineering from Xi'an Jiaotong University, China, in 1987. After a Postdoctoral Fellowship with Zhejiang University, Zhejiang, China, he joined Shenzhen Anke High-Tech Company Ltd., as a Chief Technology Officer, in 1989. He served at Anke for 16 years, then he joined Shenzhen University as the Vice President and Founded the Biomedical Engineering Branch, in 2005. His main research interests include biomedical ultrasound imaging, medical instrumentation, tissue elasticity imaging, multimodal ultrasound imaging, and image processing.

• • •

HUIYING WEN received the B.S. and M.S. degrees from the Department of Biomedical Engineering, Shenzhen University, Shenzhen, China, in 2013 and 2016, respectively. She is currently pursuing the Ph.D. degree. Her research interests include medical image processing and pattern recognition, and artificial intelligence.